Deep–Sea Research I 188 (2022) 103848

Contents lists available at ScienceDirect

Deep-Sea Research Part I

journal homepage: www.elsevier.com/locate/dsri

Macrofaunal foraminifera from a former benthic impact experiment site (IOM contract area) in the abyssal eastern Clarion-Clipperton Zone

Zofia Stachowska-Kamińska [a], Andrew J. Gooday [b,c,*], Teresa Radziejewska [a], Pedro Martínez Arbizu [d]

[a] Institute of Marine and Environmental Sciences, University of Szczecin, ul. Mickiewicza 16A, 70-383, Szczecin, Poland
[b] National Oceanography Centre, Southampton, European Way, Southampton, SO14 3ZH, UK
[c] Life Sciences Department, Natural History Museum, Cromwell Road, London, SW7 5BD, UK
[d] German Center for Marine Biodiversity Research, Senckenberg am Meer, 26382, Wilhelmshaven, Germany

ARTICLE INFO

Keywords:
Deep-sea foraminifera
Seabed mining
Polymetallic nodules
Mining impacts
Monothalamids

ABSTRACT

We analysed macrofaunal (>250 μm) foraminifera in the 0–1 cm layer of three replicate multicorer samples collected in 2015 at each of three abyssal sites ('impacted', 'resedimented' and 'control') in the IOM contract area of the eastern Clarion-Clipperton Zone (CCZ), where a benthic impact experiment (BIE) had been conducted in 1995 in order to simulate disturbances resulting from the seabed mining of polymetallic nodules. Taxonomic composition was similar between sites, with monothalamids representing 79% of complete 'live' (Rose-Bengal-stained) tests and multichambered taxa constituting a slim majority (55% overall) of dead tests. Monothalamids comprised a mixture of formal taxa and informal morphological groupings. Komokiaceans in the family Baculellidae predominated and included the top-ranked species *Edgertonia* sp. 7. Other komokiaceans (Komokiidae) and tubular, spindle-shaped and spherical morphotypes were also common. Multichambered taxa were mainly agglutinated, uniserial hormosinids being well represented together with coiled species, notably *Cribrostomoides subglobosus* (2nd ranked species). Fragments were almost three times as abundant as complete tests and dominated by tubes (notably *Rhizammina* sp.), many of them 'live'. Our results are consistent with earlier studies showing that monothalamids, many of them undescribed, are important elements of abyssal foraminiferal assemblages in the eastern CCZ. Mean specimen counts for 'live' and dead tests (50.7–75.7 and 54.3–72.7 individuals/sample, respectively) were not significantly different between sites. Assemblages were very diverse with 43–85 morphospecies per sample and 220 in total (201–1081 specimens per sample, 4361 total), more than three-quarters of them monothalamids. Species richness and diversity were lower at the control site than at the impacted and resedimented sites, and eveness and Rank 1 dominance lowest at the resedimented site, but differences were not significant for any of these metrics. The absence of significant differences in faunal density, diversity, and taxonomic composition at impacted, resedimented and control sites 20 years after the experimental disturbance may reflect a number of factors, including insufficient sample replication.

1. Introduction

Benthic foraminifera are an immensely successful group of relatively large testate protists belonging to the supergroup Rhizaria. They are present on hard and soft substrates in marine settings from coastal and estuarine habitats to the greatest ocean depths (Murray, 2006) and make an important contribution to the biodiversity of deep-sea ecosystems (Gooday et al., 2020b). This is particularly true in abyssal habitats, including the Clarion-Clipperton Zone (CCZ), a vast region of the central equatorial Pacific extending for a distance of about 4,200 km from 115° to 155° W at depths of about 4000 m in the east to about 5,400 m in the west.

The CCZ is currently the focus of great interest because it hosts extensive seafloor deposits of polymetallic nodules that are of considerable economic value. Because these deposits lie in international waters, commercial activities are regulated by a U.N. body, the International Seabed Authority (ISA), which has negotiated contracts with 19 companies and other entities that permit them to conduct

* Corresponding author. National Oceanography Centre, Southampton, European Way, Southampton, SO14 3ZH, UK.
E-mail address: ang@noc.ac.uk (A.J. Gooday).

https://doi.org/10.1016/j.dsr.2022.103848
Received 25 April 2022; Received in revised form 15 July 2022; Accepted 20 July 2022
Available online 31 July 2022

baseline environmental studies and prospecting activities within designated areas of seafloor, up to 75,000 km^2 in extent. The baseline studies have included research on benthic foraminifera, focussed largely in the United Kingdom 1 (UK-1) and Ocean Minerals Singapore (OMS) contract areas at the eastern end of the CCZ (Goineau and Gooday, 2015, 2017, 2019; Gooday et al., 2015, 2017; Gooday and Goineau, 2019). In both areas, these protists are a common and diverse component of benthic assemblages in the meiofaunal and macrofaunal size ranges, as well as being dominant members of the megafauna across the wider CCZ (reviewed in Gooday et al., 2021).

Here, we extend these foraminiferal studies to the contract area assigned to an inter-governmental consortium, the Interoceanmetal Joint Organization (IOM), located to the west of the OMS claim. Previous research in this part of the eastern CCZ has described some features of the benthic foraminiferal assemblages in the meiofaunal size range (Radziejewska et al., 2006) and soft-bodied, macrofauna-sized monothalamous (single-chambered) foraminifera (Kamenskaya et al., 2012). Our new study is based on the macrofaunal fraction (>250 μm) of samples from an area where a benthic impact experiment (IOM BIE) was carried out in 1995 in order to simulate effects of seabed mining (Radziejewska, 2002). The experiment involved 14 tows along a pre-determined route of a special device (the Benthic Disturber; Brockett and Richards, 1994) that disturbed a nodule-free patch of the seafloor 1.5 x 2 km in extent (Fig. 1). The Disturber created furrows ~10-cm deep in the seafloor, with overturned sediment being visible on furrow flanks, and resuspended an estimated 1,800 m^3 of sediment (Radziejewska, 2014). The metazoan meiofauna analysed in cores collected from inside the furrows directly after the disturbance showed a substantial reduction of densities, whereas cores obtained from overturned sediment in their flanks showed an inverted pattern of meiofaunal vertical distribution, with densities increasing downcore. The furrows, however, did not cover the seafloor uniformly, and some undisturbed patches were left between them. Sediment trap data from moorings deployed around the tow track showed that the deposition of resuspended sediment occurred mainly in that zone. The thickness of the layer was at least 5 mm based on visual observation of cores collected immediately post-disturbance. The metazoan meiofauna was analysed prior to the disturbance and directly after it was produced, with subsequent sampling events in 1997, 2000 (Radziejewska, 2014) and 2015 (Radziejewska et al., in prep.).

Our study is based on samples collected during the most recent 2015 campaign (20 years after the disturbance) within the framework of the JPIO Ecological Aspects of Deep-Sea Mining project (Martinez Arbizu and Haeckel, 2015). Three general sites were sampled, one that was directly impacted by the disturbing device, another that was influenced by the deposition of resuspended sediment, with the third being a control site (Fig. 1). Our goal is to characterise the taxonomic composition and diversity of the larger foraminifera in these samples, and thereby to address the question of whether there was any evidence for a lasting impact of the 1995 experimental disturbance on macrofaunal foraminifera. This is an important issue given the major role that foraminifera are believed to play in the functioning of abyssal ecosystems in the CCZ (Gooday et al., 2021).

2. Materials and methods

The samples were taken in 2015 during RV SONNE cruise SO239 EcoResponse at the IOM contract area in the CCZ. The sediment was sampled with a multiple corer (or multicorer, MUC), a sampler designed to collect intact sediment cores using twelve 60-cm long, 94-mm internal diameter (i.d.) clear plastic tubes (Martínez Arbizu and Haeckel, 2015).

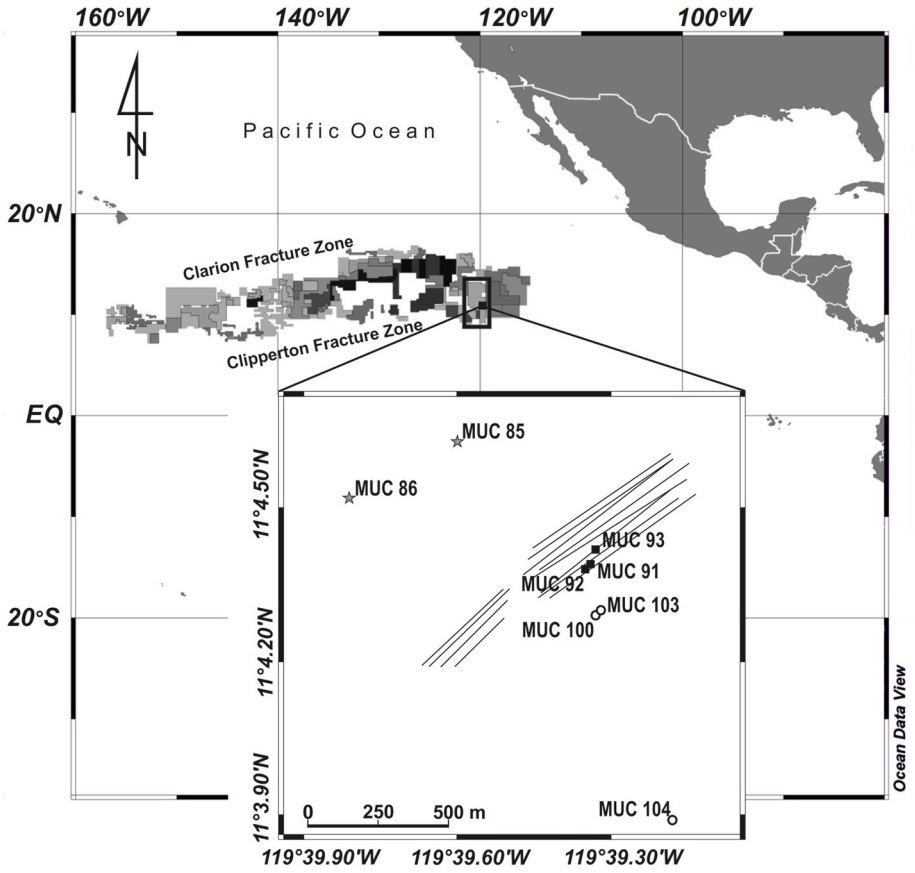

Fig. 1. Location of the former IOM BIE test site in the Clarion-Clipperton nodule field (individual contract areas marked with different shades of grey) and distribution of coring stations. Stars = control site. Solid squares = impacted site, with benthic disturber tracks (Radziejewska, 2002) shown as lines. Open circles = resedimented site. The three cores from the impacted site included two retrieved from a single MUC deployment (Core 86).

The nine samples analysed originated from eight stations (Fig. 1), with two cores being obtained from the same deployment of the MUC (station 86) at the control site (Supplementary Table S1). After retrieval, each core was processed by first removing the water overlying the sediment, passing it through a 32-μm-mesh sieve, and collecting the sieve residue in a container. The sediment core was then sliced into 0.5-cm thick layers (each about 34.7 cm^3) down to 3 cm depth in the sediment, each layer being placed in a separate container; the deeper sediment was sliced into 1 cm layers (ca. 69.4 cm^3) down to 6 cm in the sediment, each layer again being placed in a separate container. The overlying water and sediment samples were preserved with 10% borax-buffered seawater formalin. In this study, only the topmost 1 cm layer is considered.

In the on-land laboratory, the samples were stained with an aqueous solution of Rose Bengal and passed through a set of sieves with mesh sizes recommended for meiofauna research (Radziejewska, 2002), 32 μm being the lowest mesh size. These sediment residues were sorted for metazoan meiofauna as part of a separate study, following which the residues were returned to their original containers with 10% aqueous solution of borax-buffered formalin. For the present study, it was decided to focus on the >250 μm fractions from the uppermost 0–1 cm sediment layer (including the overlying water); sediment residues and the overlying water were therefore sieved again on a 250 μm screen. Rose Bengal was added to the sieving residue in order to distinguish dead specimens from those that were living at the time of collection. The residues were left to stain for 24 h before being transferred to 100 ml plastic containers and stored again in 10 ml of 10% borax-buffered formalin until they could be analysed.

To extract the foraminifera, the >250 μm fractions were re-washed on a 250 μm sieve in order to remove the stain, placed in 9-cm diameter Petri dishes and examined under a Nikon SMZ 1500 stereomicroscope with a Nikon HR Plan Apo 1x WD 54 mm lens. All the specimens, both the Rose Bengal stained and unstained and including complete individuals and fragments, were picked out and transferred to glass cavity slides with glycerol. They were hand-drawn and described, and then photographed with a microscope equipped with a Nikon Digital-Sight DS-U2 camera and NIS-Elements BR 3.2 64-bit software. The complete individuals and fragments were enumerated and assigned to taxa or morphotypes, the most important of which are briefly described and illustrated in the taxonomic appendix (Supplementary Material).

2.1. Identification of formal and informal taxa and groupings

Where possible, we assigned specimens and fragments to known foraminiferal species, or at least to higher taxa following the morphology-based classification of Kaminski (2014). All of the multichambered foraminifera, and some groups (notably the Komokiacea) currently believed to be monothalamids, could be placed in higher taxa. The Komokiacea, as originally defined by Tendal and Hessler (1977) and further developed by Schröder et al. (1988), forms a fairly coherent group, termed 'core komokiaceans' by Kamenskaya et al. (2012). The 'komoki-like' category comprises a loose grouping of species with some komokiacean features, but lacking others that are typical of the group. However, many monothalamids were more difficult to assign taxonomically. In these cases we followed the pragmatic scheme of Goineau and Gooday (2017, 2019) and Gooday and Goineau (2019), grouping species into working categories according to overall test morphology (e.g., tubes, spheres, spindles, chain-like, cushion-like). Others with irregular or complex test morphologies are impossible to force into any of these categories and are therefore grouped together as 'unclassified monothalamids'.

Foraminifera inhabiting radiolarian tests (Goineau and Gooday, 2015) were too small to be considered as part of the >250 μm fraction and therefore excluded.

2.2. Data processing

Based on the number of complete specimens and fragments per core (and per site), the percent contributions and densities (no. of individuals/10 cm^2) of each morphologically distinct entity ('morphospecies') were calculated for each 0–1 cm layer, regarded as a sample. Using the PRIMER (v. 7) software package (Clarke et al., 2014; Clarke and Gorley, 2015), the Shannon-Wiener diversity index (H′) with the natural logarithm base, Fischer α, evenness J, and Rank 1 Dominance metrics were computed (DIVERSE module) for complete individuals [stained (L) and unstained (D)] from each sample.

To analyse the composition and structure of the foraminifera assemblages, the similarity between pairs of cores across the three sampling sites (control, impacted, resedimented) was determined and similarity/dissimilarity analyses using the non-metric multi-dimensional similarity analysis (MDS) were conducted with the PRIMER SIMPER and MDS modules, respectively. The MDS ordinations were based on the Bray-Curtis similarity index and group-average sorting. The MDS analyses were performed in order to explore the similarity/dissimilarity between sites in terms of species abundances [specimen counts with log (x+1) data transformation] and the relative abundances (fourth root transformation of percentage data). Separate analyses were run on data for complete stained ('live') and complete dead individuals representing each taxon identified.

The significance of differences between the three sites in the number of taxa, assemblage abundance, and diversity (H' values), was tested using the Kruskal-Wallis test, a non-parametric analogue of the 1-way analysis of variance (ANOVA). The tests were run using the PAST (v.4) (Hammer et al., 2001).

Significance of differences in the absolute and relative abundances between the treatments was tested with the analysis of similarity and permutational analysis of variance, using the PRIMER modules ANOSIM and PERMANOVA, respectively.

Total diversity was estimated based on total specimen counts ('live + dead', 'live', and 'dead' specimens) for each site type using species rarefaction curves (Gotelli and Colwell, 2011) as well as Chao-1 (abundance-based estimation) and Chao-2 (incidence-based estimation) indices (Chao and Chiu, 2016). Rarefaction curves were developed using estimates produced by the PAST (v.4) software (Hammer et al., 2001). The species richness was estimated using Chao-1 (abundance--based) and Chao-2 (incidence-based) and plotted using data from the PLOT module of the PRIMER (v. 7) package (Clarke et al., 2014; Clarke and Gorley, 2015).

3. Results

3.1. Abundance

Among the total of 1,132 complete specimens (intact tests) sorted from the nine samples, 585 (51.7%) were judged to be 'live' (stained) when collected based on Rose Bengal staining and other criteria (e.g., general condition of test and 'freshness' of stercomata) and 547 (48.3%) were considered to be dead (Table 1). The number of specimens in individual samples ranged from 22 to 123 (stained) and 28 to 107 (dead), with an overall means of 65.0 ± 34.8 and 60.8 ± 23.1, respectively, per sample. Stained tests were more abundant than dead tests in five of the nine samples, notably so in sample 103/5 (resedimented site), which yielded almost twice as many stained (123) as dead (68) tests. There were no clear differences in the mean abundances (specimen counts) of intact tests between sites. These ranged from means of 50.7 (control site) to 75.7 (resedimented site) per sample for stained tests and 54.3 (resedimented) to 72.7 (impacted) for dead tests. Corresponding densities were 7.31–10.9 individuals/10 cm^2 (stained) and 7.82 to 10.5 individuals/10 cm^2 (dead). The between-sites differences in abundances of both stained and non-stained individuals proved non-significant (Kruskal-Wallis test, $p > 0.05$).

Table 1
Abundance (actual counts) and densities (per 10 cm^2) of complete tests and fragments of tests in individual samples. N = number per sample. Frag = fragment.

	Live		Lfrag		Dead		Dfrag	
	N	Density	N	Density	N	Density	N	Density
Control								
85/10	47	6.77	267	38.5	28	4.03	69	9.94
86/2	81	11.7	328	47.2	63	9.07	104	15.0
86/3	24	3.46	47	6.77	75	10.8	68	9.80
Mean	50.7	7.31	214	30.8	55.3	7.97	80.3	11.6
S.D.	28.6	4.15	148	21.3	24.4	3.52	20.5	2.96
Impacted								
91/12	86	12.4	194	27.9	107	15.4	77	11.1
92/2	98	14.1	347	50.0	42	6.05	224	32.3
93/10	22	3.17	27	3.89	69	9.93	83	12.0
Mean	68.7	9.89	189	27.3	72.7	10.5	128	18.5
S.D.	40.9	5.88	160	23.1	32.7	4.70	83.2	12.0
Resedimented								
100/6	65	9.36	381	54.9	45	6.48	102	14.7
103/5	123	17.7	630	90.7	68	9.79	260	37.4
104/10	39	5.62	99	14.26	50	7.20	42	6.05
Mean	75.7	10.9	370	53.3	54.3	7.82	134	19.4
S.D.	43.0	6.18	266	38.2	12.1	1.74	113	16.2
Total (including indet.)	**585**		**2320**		**547**		**1029**	
Indeterminate (N)	22		63		28		106	
Indeterminate (%)	3.76		3.72		5.12		10.3	
Mean	**65.0**	**9.37**	**258**	**37.1**	**60.8**	**8.75**	**114**	**16.5**
S.D.	**34.8**	**5.01**	**192**	**27.6**	**23.1**	**3.32**	**75.3**	**10.8**

Overall, test fragments were almost three times as abundant as complete tests. Of the 3,349 fragments recovered, 2,320 (69.3%) were stained and 1,029 (30.7%) were considered to be dead (Table 1). Abundances per site were consistently higher among stained fragments and also higher in all but two individual samples. However, there was considerable variation in the number of fragments between samples at each site, particularly in the case of those that were stained. These ranged from 47 to 328 (control), 27 to 347 (impacted) and 99 to 630 (resedimented).

Complete foraminiferal tests (both 'live' and dead) were more common in the upper layer (top water + 0–0.5 cm) at the impacted and resedimented sites, typically by a factor of 2, but more common in the lower layer (0.5–1.0 cm) at the control site (Supplementary Table S2). 'Live' and dead fragments, however, were more common in the upper layer at all three sites.

3.2. Taxonomic composition

Assemblages of complete tests included both multichambered (classes Globothalamea and Tubulotalamea) and single-chambered (class Monothalamea, i.e., monothalamids) groups (Table 2). At individual sites and overall, dead multichambered tests were more common than stained multichambered tests, accounting for 49.7–58.8% of the total (i.e., 'live' + dead) assemblage (55.8% overall) compared to only 21% of the stained assemblage. Conversely, the monothalamids represented more than 76% of the 'live' assemblages at all sites (79% overall) compared to 50% or less of the dead assemblage (44.2% overall). This difference reflects the generally greater fragility of monothalamids compared to most multichambered taxa. Although the absolute and relative abundance of the different groups varied somewhat between samples, the general composition of the assemblages was consistent across the sites.

Multichambered taxa comprised mainly textulariids (agglutinated Globothalamea), among which uniserial hormosinids (species of *Hormosina, Hormosinella,* and *Reophax*; Supplementary Fig. S2) were an important element, together with the coiled lituolid *Cribrostomoides subglobosus* (Supplementary Fig. S3E). Calcareous species were always rare, being represented by occasional rotaliids (Globothalamea) and miliolids (Tubulothalamea). The tests of rotaliids were always dissolved leaving only the cell body, or in the case of dead individuals the inner organic lining. This makes species identification impossible, although some specimens can probably be assigned to the genus *Cibicidoides*. Miliolids were represented by occasional partly dissolved tests of *Pyrgoella irregularis* (sensu Enge et al. (2012). Dead specimens of *Ammodiscus* (Supplementary Fig. S1) (agglutinated Tubulothalamea) were fairly common.

Monothalamids comprise a mixture of formal taxa and informal morphology-based groupings (Table 2). In most samples, specimens considered to be 'live' usually outnumbered those that were dead. Saccamminids (dead 4.04% vs 'live' 1.54%) were an exception, mainly due to relatively large numbers of a *Saccammina* species with a rigid, fairly robust test that was represented only by dead specimens (Fig. 3A–C). Overall, the Komokiacea (Supplementary Figs. S6–8), mainly species of the family Baculellidae, were the most abundant group, with the two constituent families together contributing more than 42% of the 'live' and almost 21% of the dead assemblage. A variety of spheres (Supplementary Fig. S11), spindles, and particularly tubes (Fig. 4; Supplementary Figs. S9 and 10) were also fairly common, together with unclassified monothalamids (Fig. 3F–H; Supplementary Figs. S9–11).

Tubes contributed a large and consistent majority (80.0–80.5%; 81.9% overall) of the 'live' test fragments (Table 3). Komokiaceans and unclassified monothalamids made modest contributions, while the uniserial and often delicate hormosinids were the only multichambered group that fragmented to any extent.

3.3. Multivariate analyses

Exploration of the species abundance structure of both stained and non-stained complete individuals using multivariate analyses yielded the following results. First, there was a low overall mean similarity between pairs of cores across the three groups of sites (28.79 ± 6.01% and 38.54 ± 6.90% for stained and non-stained individuals, respectively; SIMPER). Second, there were no significant differences in the species abundance structure between the treatments, as indicated by the results of ANOSIM and PERMANOVA (Table 4). Third, the MDS plots did not show any obvious grouping of individual cores according to the samping site (control, impacted, or resedimented) (Fig. 2A and B).

As in the case of species abundance, the structure of the relative

Table 2
Absolute and relative (%) abundance of major taxa and groupings based on complete tests. The abundances and percentages in the two 'Total' rows are based on the totals of the three samples combined. This provides an integrated view of the faunal composition at each site. L = 'Live' (stained). D = Dead. L + D stained + dead combined. Sample numbers are given in parentheses in top row (note that 2 samples were taken at Station 86).

Morphological groupings	Control site (85, 86)						Impacted site (91, 92, 93)						Resedimented site (100,103,104)						3 sites					
	L	%L	D	%D	L + D	%L + D	L	%L	D	%D	L + D	%L + D	L	%	D	%D	L + D	%L + D	L	%	D	%D	L + D	%L + D
Multichambered																								
Rotaliids	0	0	2.0	1.20	2.0	0.63	0	0	3.0	1.39	3.0	0.71	3.0	1.33	3.0	1.84	6.0	1.54	3.0	0.51	8.0	1.47	11	0.97
Miliolids	2.0	1.31	0	0	2.0	0.63	1.0	0.49	0	0	1.0	0.24	0	0	0	0	0	0	3.0	0.51	0	0	3.0	0.27
Ammodiscids	1.0	0.65	6.0	3.61	7.0	2.19	1.0	0.49	11	5.09	12	2.84	0	0	7.0	4.29	7.0	1.80	2.0	0.34	24	4.40	26	2.30
Hormosinids	14	9.15	29	17.5	43	13.5	15	7.28	30	13.9	45	10.7	27	11.9	31	19.0	58	14.9	56	9.57	90	16.5	146	12.9
Trochamminids	0	0	6.0	3.61	6.0	1.88	1.0	0.49	23	10.6	24	5.69	2.0	0.89	3.0	1.84	5.0	1.29	3.0	0.51	32	5.87	35	3.10
Other textulariids	19	12.4	53	31.9	72	22.6	18	8.74	60	27.8	78	18.5	19	8.41	37	22.7	56	14.4	56	9.57	150	27.5	206	18.2
Total multichambered	**36**	**23.5**	**96**	**57.8**	**132**	**41.4**	**36**	**17.5**	**127**	**58.8**	**163**	**38.6**	**51**	**22.6**	**81**	**49.7**	**132**	**33.9**	**123**	**21.0**	**304**	**55.8**	**427**	**37.8**
Monothalamids																								
Nodellum-like	0	0	0	0	0	0	0	0	2.0.0	0.93	2.0	0.47	0	0	0	0	0	0	0	0	2.0	0.37	2.0	0.18
Lagenamminids	2.0	1.31	2.0	1.20	4.0	1.25	2.0	0.97	3.0	1.39	5.0	1.18	4.0	1.77	1.0	0.61	5.0	1.29	8.0	1.38	6.0	1.10	14	1.24
Flasks	2.0	1.31	0	0	2.0	0.63	0	0	1.0	0.46	1.0	0.24	0	0	0	0	0	0	2.0	0.34	1.0	0.18	3.0	0.27
Saccamminids	1.0	0.65	8.0	4.82	9.0	2.82	4.0	1.94	1.0	0.46	5.0	1.185	4.0	1.77	13	7.98	17	4.37	9.0	1.54	22	4.04	31	2.74
Spheres	7.0	4.58	4.0	2.41	11	3.45	12	5.83	7.0	3.24	19	4.50	14	6.20	5.0	3.07	19	4.88	33	5.64	16	2.94	49	4.34
Organic-walled	1.0	0.65	0	0	1.0	0.31	0	0	0	0	0	0	0	0	0	0	0	0	1.0	0.17	0	0	1.0	0.09
Hyperamminids	2.0	1.31	2.0	1.20	4.0	1.25	1.0	0.49	0	0	1.0	0.24	2.0	0.88	1.0	0.61	3.0	0.77	5.0	0.85	3.0	0.55	8.0	0.71
Tubes	13	8.50	8.0	4.82	21	6.58	20	9.71	14	6.48	34	8.06	16	7.08	22	13.5	38	9.77	49	8.38	44	8.07	93	8.23
Spindles	22	14.4	0	0	22	6.90	8.0	3.88	5.0	2.31	13	3.08	19	8.41	5.0	3.07	24	6.17	49	8.38	10	1.83	59	5.22
Chain-like	0	0	0	0	0	0	2.0	0.97	1.0	0.46	3.0	0.71	4.0	1.77	1.0	0.61	5.0	1.29	6.0	1.03	2.0	0.37	8.0	0.71
Unclassified	10	6.54	3.0	1.81	13	4.08	9.0	4.37	0	0	9.0	2.13	7.0	3.10	2.0	1.23	9.0	2.31	26	4.44	5.0	0.92	31	2.74
Cushion-like	0	0	1.0	0.60	1.0	0.31	4.0	1.94	1.0	0.46	5.0	1.18	1.0	0.44	1.0	0.61	2.0	0.51	5.0	0.85	3.0	0.55	8.0	0.71
Komokiacean-like	0	0	0	0	0	0	7.0	3.40	4.0	1.85	11	2.61	11	4.87	9.0	5.52	20	5.14	18	3.08	13	2.39	31	2.74
Komokiacea:																								
- Baculellidae	51	33.3	35	21.1	86	27.0	80	38.8	40	18.5	120	28.4	69	30.5	14	8.59	83	21.3	200	34.2	89	16.3	289	25.6
- Komokiidae	6.0	3.92	7.0	4.22	13	4.08	21	10.2	10	4.63	31	7.35	22	9.73	8.0	4.91	30	7.71	49	8.38	25	4.59	74	.55
Indeterminate	0	0	0	0		0	0	0	0	0	0	0	2.0	0.88	0	0	2.0	0.51	2.0	0.34	0	0	2.0	0.18
Total monothalamids	**117**	**76.5**	**70**	**42.2**	**187**	**58.6**	**170**	**82.5**	**89**	**41.2**	**259**	**61.4**	**175**	**77.4**	**82**	**50.3**	**257**	**66.1**	**462**	**79.0**	**241**	**44.2**	**703**	**62.2**
Grand Total	**153**		**166**		**319**		**206**		**216**		**422**		**226**		**163**		**389**		**585**		**545**		**1130**	

Table 3
Absolute and relative (%) abundance of major taxa and groupings based on test fragments. The abundances and percentages in the two 'Total' rows are based on the totals of the three samples combined. This provides an integrated view of the faunal composition of fragments at each site. L = 'Live' (stained). D = Dead. L + D stained + dead combined. Multi. = multichambered. Mono. = monothalamids. Sample numbers are given in parentheses in top row (note that 2 samples were taken at Station 86).

Morphological groupings	Control site (85, 86)						Impacted site (91, 92, 93)						Resedimented site (100,103,104)						3 sites					
	Lfr	%	Dfr	%	Tot	%	Lfr	%	Dfr	%	Tot	%	Lfr	%	Dfr	%	Tot	%	Lfr	%	Dfr	%	Tot	%
Multichambered																								
Rotaliids	0	0	0	0	0	0	0	0	0	0	0	0	0	0	0	0	0	0	0	0	0	0	0	0
Miliolids	0	0	0	0	0	0	0	0	0	0	0	0	0	0	0	0	0	0	0	0	0	0	0	0
Ammodiscids	0	0	1.00	0.40	1.00	0.11	0	0	1.00	0.24	1.00	0.24	1.00	0.10	1.00	0.26	2.00	0.13	1.00	0	3	0.29	4.00	0.12
Hormosinids	10.0	1.56	42.0	16.9	52.0	5.82	10.0	1.77	53.0	12.6	63.0	12.6	22.0	6.38	57.0	14.8	79.0	5.25	42.0	1.80	152	14.6	194	5.73
Trochamminids	0	0	0	0	0	0	2.00	0.35	1.00	0.24	3.00	0.24	0	0.30	0	0	0	0	2.00	0.09	1.00	0.10	3.00	0.09
Other textulariids	1	0.17	6.00	2.41	7.00	0.78	2.00	0.35	7.00	1.67	9.00	1.67	1.00	0.91	0	0	1.00	0.07	4.00	0.17	13.0	1.25	17.0	0.50
Total Multi.	**11.0**	**1.71**	**49.0**	**19.7**	**60.0**	**6.72**	**14.0**	**2.47**	**62.0**	**14.7**	**76.0**	**14.7**	**24.0**	**7.70**	**58.0**	**15.1**	**82.0**	**5.44**	**49.0**	**2.06**	**169**	**16.3**	**218**	**6.44**
Monothalamids																								
Nodellum-like	0	0	0	0	0	0	0	0	2	0.48	2.00	0.48	0	0.20	0	0	0	0	0	0	2.00	0.19	2.00	0.06
Lagenamminids	0	0	0	0	0	0	0	0	0	0	0	0	0	0	0	0	0	0	0	0	0	0	0	0
Flasks	0	0	0	0	0	0	0	0	0	0	0	0	0	0	0	0	0	0	0	0	0	0	0	0
Saccamminids	0	0	2.00	0.80	2.00	0.22	0	0	0	0	0	0	0	0	2	0.52	2.00	0.13	0	0	4.00	0.39	4.00	0.12
Spheres	5.00	0.79	6.00	2.41	11.0	1.23	0	0	10.0	2.38	10.0	2.38	5.00	1.01	12.0	3.12	17.0	1.13	10.0	0.43	28.0	1.16	38.0	1.12
Organic-walled	0	0	0	0	0	0	1.00	0.18	0	0	1.00	0	0	0.11	0	0	0	0	1.00	0.04	0	0	1.00	0.03
Hyperamminids	8.00	1.24	17.0	6.83	25.0	2.80	8.00	1.41	5.00	1.19	13.0	1.19	11.0	1.32	11.0	2.86	22.0	1.46	27.0	1.16	33.0	3.18	60.0	1.77
Tubes	531	82.5	136	54.6	667	74.7	453	80.0	251	59.6	704	59.6	925	82.4	188	49.0	1113	73.9	1909	81.9	575	55.4	2484	73.4
Spindles	1.00	0.16	0	0	1.00	0.11	8.00	1.41	3.00	0.71	11.0	0.71	16.0	1.11	0	0	16.0	1.06	25.0	1.07	3.00	0.29	28.0	0.83
Chain-like	3.00	0.47	5.00	2.01	8.00	0.90	1.00	0.18	1.00	0.24	2.00	0.24	5.00	0.20	46.0	10.0	51.0	3.39	9.00	0.39	52.0	5.01	61.0	1.80
Unclassified	17.0	2.64	0	0	17.0	1.90	21.0	3.72	0	0	21.0	0	35.0	2.13	0	0	35.0	2.32	73.0	3.13	0	0	73.0	2.16
Cushion-like	1.00	0.16	0	0	1.00	0.11	0	0	0	0	0	0	7.00	0	1.00	0.26	8.00	0.53	8.00	0.34	1.00	0.10	9.00	0.27
Komoki-like	0	0	3.00	1.20	3.00	0.34	2.00	0.35	2.00	0.48	4.00	0.48	0	0.41	4.0	1.04	4.00	0.27	2.00	0.09	9.00	0.87	11.0	0.32
Baculellidae	9.00	1.40	20.0	8.03	29.0	3.25	11.0	1.94	37.0	8.79	48.0	8.79	17.0	4.86	22.0	5.73	39.0	2.59	37.0	1.59	79.0	7.61	116	3.43
Komokiidae	37.0	5.75	8.00	3.21	45.0	5.04	47.0	8.30	48.0	11.4	95.0	11.4	77.0	9.63	40.0	10.4	117	7.77	161	6.91	96.0	9.25	257	7.59
Indeterminate	21.0	3.26	3.00	1.20	24.0	2.69	0	0	0	0	0	0	0	0	0	0	0	0	21.0	0.9	3.00	0.29	24.0	0.71
Total Mono.	**633**		**200**		**833**		**552**		**359**		**911**		**1098**		**326**		**1424**		**2283**		**885**		**3168**	
Grand Total	**644**		**249**		**893**		**566**		**421**		**987**		**1122**		**384**		**1506**		**2331**		**1038**		**3386**	

Table 4
ANOSIM and PERMANOVA tables for abundances and relative abundances of complete tests.

Analysis	Variable			
	Abundance, log(x+1)-transf. Live (stained)	Abundance, log(x+1)- transf. Dead	Relative abundance, 4th root-transf. Live (stained)	Relative abundance, 4th root-transf. , Dead
ANOSIM				
Global R (sample statistic)	−0.078	−0.111	−0.128	−0.111
Significance level (%) of sample statistic	66.1	80.7	77.9	77.9
No. of permutations	280 (all possible permutations)	280 (all possible permutations)	280 (all possible permutations)	280 (all possible permutations)
PERMANOVA				
Pseudo-F	0.88938	0.91301	0.92194	0.94297
Significance level	0.745	0.688	0.705	0.603
No. of unique permutations	273	272	274	273

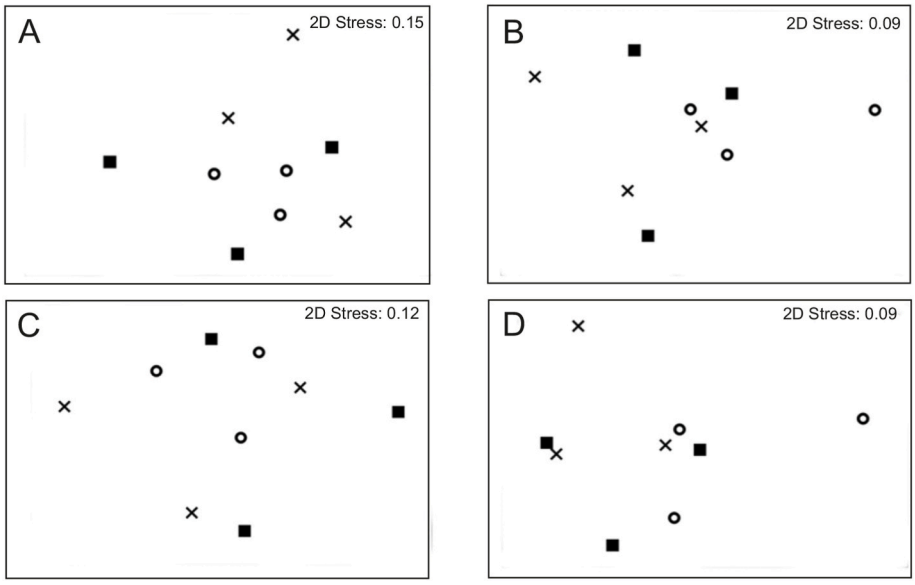

Fig. 2. MDS plots based on assemblages of complete individuals. Similarity of species abundance structure (A, 'live'; B, dead) and of relative (%) species abundance structure (C, 'live'; D, dead) Crosses = control site. Solid squares = impacted site. Open circles = resedimentated site.

species abundances (%) based on complete individuals, both stained and dead, showed only a low degree of similarity between pairs of stations across the data set (29.65 ± 5.99% and 40.03 ± 7.38% for stained and non-stained individuals, respectively; SIMPER). The lack of any significant differences between sites was also shown by the results of ANOSIM and PERMANOVA analyses (Table 4). Similarly, cores from the three main sites (control, impacted, resedimented) showed no obvious associations that would indicate differences between the them in MDS plots (Fig. 2C and D).

3.4. Species rankings

The 24 top-ranked species among the stained and dead assemblages of specimens considered to be complete or more or less complete (combined data from all samples from all sites) are listed in Table 5. They are briefly described and in most cases illustrated either in the taxonomic appendix (Supplementary material) or in Fig. 3. More than two-thirds (17 out of 24) of the more common stained species were monothalamids, 12 of them komokiaceans (assumed to be monothalamids). In comparison, only half (12 out of 24) of the more common dead species were monothalamids, and only 5 were komokiaceans. Conversely, 7 of the top 24 stained species were multichambered globothalamids (agglutinated lituolids and hormosinids) compared to 14 of the top 26 among the dead species. The total (stained plus dead) assemblage comprised proportions of the main groups that are intermediate between those of the stained and dead assemblages (Table 6). Ammodiscids only appeared among the top 24 in the dead (2 species) and total (1 species) assemblages. The widely distributed lituolid *Cribrostomoides subglobosus* (Supplementary Fig. S3E), and the komokiacean *Edgertonia* sp. 7 (Fig. 3D and E), were consistently the two most abundant species in the stained, dead and total assemblages.

Unambiguously fragmented species were dominated by *Rhizammina* sp. (38.8% of stained plus dead fragments combined) (Fig. 4A) and an undescribed, sparsely branched form (20.8%) filled with brightly stained cytoplasm and with numerous spicules projecting from the test wall (Fig. 4B). The vast majority (98.0% and 88.9%, respectively) of fragments of these two species were stained. On the other hand, an undescribed tubular form (Fig. 4C) that is ranked 3rd (9.69%) was mainly represented by dead fragments (95.0%), while another tubular form (Fig. 4D), ranked 5th, was represented by approximately equal proportions of stained and dead fragments. The 4th-ranked species (2.66%) is a *Baculella*-like komokiacean (Supplementary Fig. S6H). *Hormosinella distans,* a widely-reported homosinid, was the most common multichambered species among the fragments and ranked 7th (1.75%) overall.

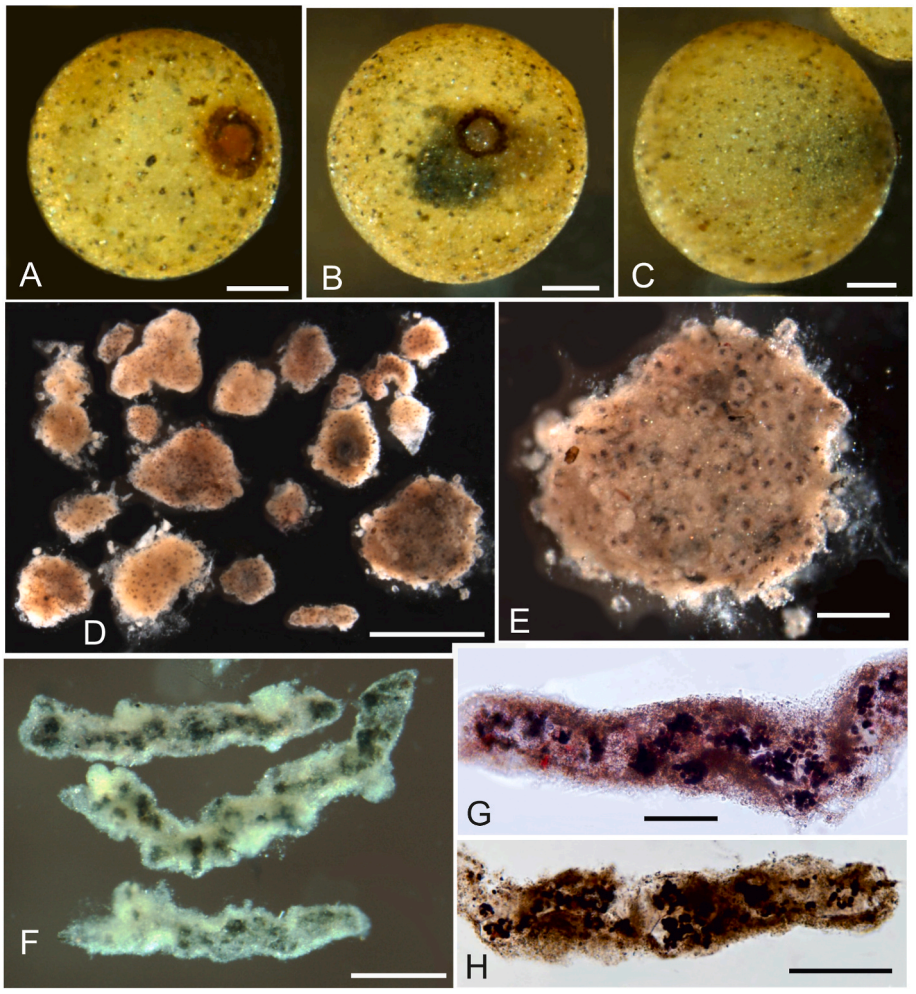

Fig. 3. Selected morphospecies. A-C) *Saccammina* sp.; Station 86-2, 0–0.5 cm layer. D–E) *Edgertonia* sp. 7; Station 86/2, 0–0.5 cm layer. F–H) Elongate compartmentalised tests; Station 103/5, 0–0.5 cm layer. Scale bars = 100 (A–C), 0.5 mm (D), 0.25 mm (E–H).

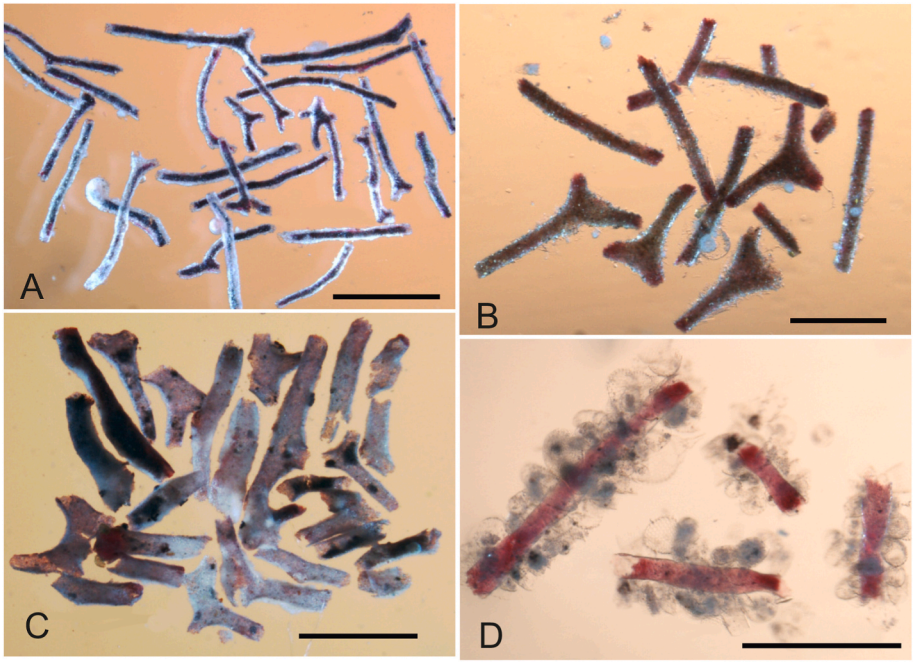

Fig. 4. Selected tubular morphospecies represented by fragments. A) Tubes of *Rhizammina* sp., 1st-ranked fragmented species; Station 100/6, 0–0.5 cm layer. B) Undescribed tubes with projecting spicules, 2nd-ranked fragmented species; Station 92/2, overlying water. C) Undescribed tubes, 3rd-ranked fragmented species; Station 92/2, 0.5–1.0 cm. D) Undescribed tubes with stained cytoplasm inside organic tube studded with radiolarians, 4th-ranked fragmented species; Station 92/2, overlying water. Scale bars = 1 mm (A,C); 0.5 mm (B,D).

Table 5
Twenty-four top-ranked species among the 'live' and dead assemblages. N = total number of specimens (all samples combined). Psamm = psammosphaerid.

Rank	'Live' (stained)	N	Group	Dead	N	Group
1	*Edgertonia* sp. 7	87	Komokioidea: Baculellidae	*Cribrostomoides subglobosus*	86	Globothalamea: Lituolida
2	*Cribro. subglobosus*	36	Globothalamea: Lituolida	*Edgertonia* sp. 7	36	Komokioidea: Baculellidae
3	Elongate, compartmentalised	31	?Monothalamea: spindle	*Baculella*-like	31	Komokioidea: Baculellidae
4	*Baculella globofera*	26	Komokioidea: Baculellidae	*Reophax* sp. 1	27	Globothalamea: hormosinid
5	*Baculella* sp. 1	21	Komokioidea: Baculellidae	*Hormosina* sp. 1	22	Globothalamea: hormosinid
6	Dark, elongate spindle	19	?Monothalamea: spindle	*Reophax* sp. 5	20	Globothalamea: hormosinid
7	Cluster organic-walled flasks	16	Komoki-like	*Saccammina* sp.	19	Monothalamea: Saccamminid
8	*Hormosina* sp. 1	14	Globothalamea: hormosinid	*Ammodiscus anguillae*	13	Tubulothalamea:Ammodiscida
9	*Reophax* sp. 1	13	Globothalamea: hormosinid	*Ammobaculites agglutinans*	13	Globothalamea: Lituolida
9	Red tube with constrictions	13	Monothalamea: Tube	Planispiral lituolid sp. 1	12	Globothalamea: Lituolida
9	Mudball species 1	13	Komokioidea: Komokiidae	Mudball species 2	12	Komokioidea: Baculellidae
9	*Edgertonia floccula*	13	Komokioidea: Baculellidae	*Baculella globofera*	12	Komokioidea: Baculellidae
13	Mudball species 2	12	Komokioidea: Komokiidae	Cluster organic-walled flasks	11	Komoki-like
14	*Reophax* sp. 5	8	Globothalamea: hormosinid	*Cystammina galatea*	10	Globothalamea: Lituolida
14	*Baculella* sp. 1A	8	Komokioidea: Baculellidae	Delicate tube in radiolarian	9	Monothalamea: Tube
14	*Baculella*-like	8	Komokioidea: Baculellidae	*Adercotryma* sp.	8	Globothalamea: Lituolida
17	Delicate tube in radiolarian	7	Monothalamea: Tube	*Ammodiscus tenuis*	7	Tubulothalamea:Ammodiscida
17	*Baculella hirsuta*	7	Komokioidea: Baculellidae	*Trochammina* sp. 1	7	Globothalamea: Lituolida
17	*Ammobaculites agglutinans*	6	Globothalamea: Lituolida	?*Verneuilina propinqua*	6	Globothalamea: Lituolida
20	*Hormosinella* sp. 1	6	Globothalamea: hormosinid	*Saccorhiza* sp.	6	Monothalamea: Tube
20	*Reticulum* sp.	6	Komokioidea: Komokiidae	*Baculella* sp. 1	6	Komokioidea: Baculellidae
20	*Reticulum* small mudball	6	Komokioidea: Komokiidae	'*Cyclammina*' aff. *bradyi*	5	Globothalamea: Lituolida
20	*Baculella* sp. 2 Type A.	6	Komokioidea: Baccullelidae	*Thurammina* spp.	5	Monothalamea: Psamm.
20	?*Verneuillinella propinqua*	5	Globothalamea: Lituolida	Dark elongate spindle	5	Monothalamea: spindle

Table 6
Twenty-four top-ranked species: stained and dead combined.

Rank	'Live' (stained) + Dead	Number	Group
1	*Edgertonia* sp.	123	Komokioidea: Baculellidae
2	*Cribrostomoides subglobosus*	122	Globothalamea: Lituolida
3	*Reophax* sp.	40	Globothalamea: Hormosinoidea
4	*Baculella*-like	39	Komokioidea: Baculellidae
5	*Baculella globofera*	38	Komokioidea: Baculellidae
6	*Hormosina* sp. 1	36	Globothalamea: Hormosinoidea
7	*Reophax* sp. 5	28	Globothalamea: Hormosinoidea
7	Elongate compartmentalised test	28	?Monothalamea: Spindle
9	Cluster, organic-walled flasks	27	Komoki-like
9	*Baculella* sp. 1	27	Komokioidea: Baculellidae
11	Mudball species 2	24	Komokioidea: Komokiidae
12	*Saccammina* sp.	20	Monothalamea: Saccamminidae
12	Dark, elongate spindle	20	?Monothalamea: Spindle
14	*Ammobaculites agglutinans*	19	Globothalamea: Lituolida
15	Delicate tube inside radiolarian	16	Monothalamea: Tube
16	Planispiral lituolid sp. 1	14	Globothalamea: Lituolida
16	Red tubes with constrictions	14	Monothalamea: Tube
16	Mudball species 1	14	Komokioidea: Komokiidae
16	*Edgertonia floccula*	14	Komokioidea: Baculellidae
20	*Ammodiscus anguillae*	13	Tubulothalamea:Ammodiscida
20	*Cystammina galatea*	11	Globothalamea: Lituolida
22	?*Verneuillinella propinqua*	11	Globothalamea: Lituolida
22	*Adercotryma* sp.	10	Globothalamea: Lituolida
24	*Hormosinella* sp. 1	10	Globothalamea: Hormosinoidea

3.5. Species richness and diversity

We recognised a total of 220 species (stained, dead, complete and fragmented), of which 48 (21.8%) were multichambered and 172 (78.2%) were monothalamids (Table 7). Among the multichambered taxa, hormosinids (19 species) and 'other textulariids' (16 species excluding trochamminids) included the majority of species. Among the monothalamids, tubes (55 species), spheres (22 species), komokiaceans (Komokiidae 21 and Baculellidae 19 species), and unclassified monothalamids (18 species) were the main contributors. More multichambered species were represented by dead than by stained specimens (complete and fragmented) at all three sites, while the opposite applied in the case of the monothalamids, except for fragments at the impacted site.

The total numbers of species per sample ranged from 43 to 67 at the control site (109 in total), 50 to 74 at the impacted site (122 in total) and 44 to 85 at the resedimented site (126 in total) (Table 8). The lower richness at the control site was evident among complete specimens, as shown by rarefaction curves (Fig. 5), and to a lesser extent among fragments. There were generally more stained species than dead species, with the exception of sample 86/3 (control site), where 28 species were represented by dead specimens compared to only 9 by 'live' specimens, and sample 104/10 (control site), where the numbers were equal (22). Despite these differences, the between-sites differences in species richness of both stained and non-stained individuals proved non-significant (Kruskal-Wallis test, $p > 0.05$). Rarefied species richness [($E(S_{100})$], Evenness (J') and diversity measures (Shannon-Wiener and Fischer α) were consistently highest at the resedimented site and lowest at the

Table 7
Number of species, based on combined samples in each category, belonging to major taxa/morphological groupings. L = 'Live' (stained). Lfr = 'Live' (stained) fragments. D = Dead. Dfr = Dead fragments. L + D = 'Live' (stained) + Dead combined.

Morphological groupings	Site																		Combined	
	Control						Impacted						Resedimented							
	L	Lfr	D	Dfr	L + D	Tot	L	Lfr	D	Dfr	L + D	Tot	L	Lfr	D	Dfr	L + D	Tot	Grand Total	%
Multichambered																				
Rotaliids	0	0	1	0	1	1	0	0	1	0	1	1	2	0	1	0	2	2	2	
Miliolids	1	0	0	0	1	1	1	0	0	0	1	1	0	0	0	0	0	0	1	
Ammodiscids	1	0	2	0	2	2	1	0	3	1	3	3	0	0	1	1	2	2	3	
Hormosinids	6	6	8	8	10	15	7	5	8	10	9	15	10	6	9	10	14	17	19	
Trochamminids	0	0	2	0	2	2	0	1	5		5	5	1	0	2	0	2	2	7	
Other textulariids	5	1	10	3	11	12	6	2	7	3	10	10	4	1	10	0	10	10	16	
Total multichambered species	**13**	**7**	**23**	**11**	**27**	**37**	**15**	**8**	**24**	**14**	**29**	**35**	**17**	**7**	**23**	**11**	**30**	**33**	**48**	**21.8**
Monothalamids																				
Nodellum-like	0	0	0	0	0	0	0	0	1	1	1	1	0	0	0	0	0	0	1	
Lagenamminids	1	0	0	0	0	0	1	0	3	0	4	4	2	0	1	0	2	2	5	
Flasks	0	0	0	0	0	0	0	0	0	0	0	0	0	0	0	0	0	0	0	
Saccamminids	1	0	1	1	2	2	4	0	1	1	4	4	2	0	3	1	5	5	6	
Spheres	7	0	3	1	9	9	7	0	4	2	11	11	9	0	5	4	13	15	22	
Organic-walled	1	0	0	0	1	1	0	1	0	0	1	1	0	0	0	0	0	0	2	
Hyperamminids	2	1	1	3	3	3	1	1	0	0	1	2	1	1	1	1	1	1	3	
Tubes	8	17	5	18	10	29	11	13	6	12	15	25	8	17	9	14	13	21	55	
Spindles	2	1	0	0	2	2	2	1	2	1	2	2	3	3	1	0	3	3	4	
Chain-like	0	2	0	2	0	3	1	0	1	1	2	3	2	3	1	2	3	5	8	
Unclassified	4	2	0	0	4	6	3	2	0	0	3	5	4	2	1	0	5	6	18	
Cushion-like	0	1	1	0	1	1	2	0	1	0	0	2	1	1	1	1	2	2	3	
Komokiacean-like	0	0	0	1	0	1	1	1	0	1	1	1	2	0	3	1	4	5	5	
Komokiacea: Baculellidae	10	5	6	3	11	11	9	4	5	7	9	11	10	10	2	3	10	14	19	
Komokiacea: Komokiidae	4	4	2	2	5	9	5	5	2	5	5	11	8	7	5	4	9	12	21	
Total monothalamid species	**40**	**33**	**19**	**31**	**48**	**77**	**47**	**28**	**26**	**31**	**59**	**83**	**52**	**44**	**33**	**31**	**70**	**91**	**172**	**78.2**
Grand Total of species																			**220**	

control site, except for Fischer α, which was marginally highest at the impacted site (Table 8). The difference between sites was also less pronounced for H′ based on total ('live' + dead) assemblages. Conversely, Rank 1 Dominance (R1D) values were always lowest at the resedimented site and highest at one of the two other sites. Nevertheless, the between-sites differences in richness, H′, Fischer α, J′ and R1D were non-significant (Kruskal-Wallis test, $p > 0.05$) in both stained and non-stained individuals.

These results are supported by total diversity estimates (Fig. 5 and Supplementary Figs. 12 and 13). The rarefied species richness for 'live + dead' was always highest at the resedimentated site, particularly for the total ('live + dead') assemblage, with almost no distinction between the resedimentation and impacted sites being seen in the 'live' and 'dead' assemblages. The two Chao indices were similarly consistent with this pattern.

4. Discussion

4.1. Practical challenges

The analysis of foraminifera in CCZ samples poses considerable difficulties, notably regarding the recognition of fragments and the distinction between stained and dead tests. These problems are outlined by Goineau and Gooday (2017) and discussed further in Supplementary Material 1 of Gooday and Goineau (2019). They are particularly acute in the case of monothalamids.

The designation of a specimen as a fragment depends on the recognition of one or more broken test surfaces. These are usually clearly visible in the case of multichambered taxa. Some monothalamids also display clear evidence of breakage, but in others the signs are less obvious. For example, breakage is difficult to detect in chain-like formations where segments are joined by narrow necks. In the case of tubes, it is not always clear whether one or both of the ends are fractured or original apertures. Soft-bodied komokiaceans (komoki) do not fracture but they may be broken apart during sieving. In the central North Pacific, Bernstein et al. (1978) considered that 'their extreme fragility makes routine sorting unfeasible and renders quantification almost meaningless'. However, in our experience, some komoki seem to survive the rigors of sieving in reasonable condition. Some of these, including *Baculella* species (e.g., *B. globofera* and particularly *B. hirsuta*) and the more robust types of mudball, have tests with distinct shapes and are fairly easy to recognise as intact specimens. On the other hand, species of *Reticulum* and *Lana,* which comprise a loose system of fine tubules, often lack any clear overall shape (Supplementary Fig. S7A), although some tightly-reticulated *Reticulum* species have more distinct morphologies.

The distinction between specimens that were living when collected and those that were dead is most problematic in the case of the many monothalamids that accumulate stercomata and have only sparse cytoplasm; many komokiaceans, for example, do not stain. In such cases, deciding if a specimen is 'live' or dead has to be based to a large extent on its general condition, including whether or not it is fragmented and whether the stercomata are 'fresh' or decayed into a grey powder. How long delicate monothalamid tests persist in deep-sea oxic sediments is unknown. They are certainly destroyed more rapidly than robust, multichambered taxa (Schröder, 1986) and are rarely found as fossils. However, the presence of dead komoki fragments at depths of 10 cm in multicores from the NE Atlantic (A.J Gooday, unpublished observations) suggest that some macrofaunal-sized tests could possibly survive for some decades.

Decisions about fragmentation and whether specimens were 'live' or dead are often difficult, sometimes subjective, and will not always be correct. In this study we have tried to be as careful as possible, but mistakes have undoubtedly occurred. However, we are confident that mistakes will not have substantially altered the overall description of the assemblage characteristics at our study sites.

The large proportion of undescribed species and higher taxa in our material creates further challenges. Again, this applies particularly to

Table 8
Diversity metrics including all taxa and morphology-based groups, based on combined counts of species and specimens from each site. L + Dfr = fragments of live (stained) and dead individuals.

Site and samples	Live					Dead					Live + Dead					L + Dfr	Grand Total
	S	$E(S_{100})$	H′	α	J′	R1D (%)	S	$E(S_{100})$	H′	α	J. ’	R1D (%)	S	$E(S_{100})$	H′	α	J′	R1D (%)	S	
Control																				
85/10	21	21.0	2.272	14.57	0.7463	44.7	18	18.0	2.648	23.6	0.9163	18.5	34	34.0	2.904	24.36	0.8235	28.4	29	51
86/2	38	38.0	3.211	27.91	0.8827	19.8	24	24.0	2.852	14.36	0.8976	16.1	47	39.3	3.323	24.41	0.8632	15.4	40	67
86/3	9	9.00	1.869	5.443	0.8504	39.1	28	28.0	2.983	16.83	0.8953	18.1	31	31.0	2.917	16.01	0.8493	23.2	20	43
Samples combined	53	41.2	3.265	29.06	0.8225	19.2	47	37.9	3.318	22.32	0.8619	15.5	77	42.7	3.58	32.69	0.8241	15.7	63	109
Impacted																				
91/12	35	35.0	3.107	22.81	0.874	15.7	32	32.0	2.784	16.81	0.8032	32	55	39.6	3.333	27	0.8317	20.7	45	74
92/2	35	35.0	2.998	19.65	0.8433	24.8	23	23.0	2.906	21.64	0.9268	14.6	49	40.7	3.344	27.13	0.8592	19.6	26	68
93/10	14	14.0	2.508	18.36	0.9502	14.3	24	24.0	2.58	13.39	0.8118	34.3	36	36.0	3.052	22.74	0.8517	26.1	31	50
Samples combined	68	45.9	3.621	36.15	0.8581	17.9	53	37.2	3.285	23.25	0.8273	20.1	100	46.0	3.838	42.4	0.8334	12.1	67	122
Resedimented																				
100/6	26	26.0	2.927	17.44	0.8984	18.3	25	25.0	3.046	24.96	0.9463	11.6	42	41.3	3.362	26.45	0.8995	15.5	30	59
103/5	49	45.8	3.516	33.22	0.9035	11.6	29	29.0	3.046	21.22	0.9046	16.1	60	44.4	3.651	32.56	0.8917	8.05	51	85
104/10	22	22.0	2.858	21.8	0.9245	21.1	22	22.0	2.766	15.35	0.8949	20.4	33	33.0	3.141	19.38	0.8983	14.9	4	44
Samples combined	69	46.4	3.746	35.83	0.8847	10.5	55	43.4	3.552	30.61	0.8865	12.3	96	48.9	3.956	42.6	0.8668	9.06	66	126

Fig. 5. Rarefaction curves (upper panel) and Chao diversity estimates (lower panel) for the total (‘live + dead’) assemblages at the three sites; C, control site; I, impacted site; R, resedimented.

the monothalamids, but some of the multichambered agglutinated taxa in our samples, notably hormosinid species belonging to genera such as *Reophax, Hormosina,* and *Hormosinella,* as well as trochamminaceans, are also difficult to assign to known species. At the level of higher taxa, a well-developed classification based on test morphology exists for multichambered agglutinated foraminifera (Kaminski, 2014). For the monothalamids, we followed Goineau and Gooday (2017, 2019) and Gooday and Goineau (2019) in recognising a series of groupings based on test morphology. This approach is far from ideal and has little or no phylogenetic meaning. For example, flask-shaped saccamminids, a group that is most common in finer residues, are distributed among different monothalamid clades (Voltski and Pawlowski, 2015). The tubes include a species of *Rhizammina,* a genus that groups genetically with xenophyophores (Gooday et al., 2017) and is unlikely to be related to most of the other tubes in our collection. Despite the obvious flaws, however, these groupings at least provide a simple and pragmatic framework for ordering the large diversity of undescribed monothalamids in CCZ samples.

4.2. Comparison with previous studies

Kamenskaya et al. (2012) provide a qualitative overview of soft-bodied, macrofauna-sized foraminifera, mainly komokiaceans, chain-like and tubular morphotypes in the >250-μm and >500-μm fractions of three multicorer samples collected in the region of 11° N, 119° 40′W (4380–4410 m). Some of the 46 species illustrated by Kamenskaya et al. (2012; for example, their Figs. 1e, 2e and 3a,g, 5a) can be recognised in our material. All sediment layers between 0-0.5 cm and 2.5–3.0 cm and from 3.0-4.0 cm to 5.0–6.0 cm were included. The

largest number of species was recorded in the upper three layers (0–1.5 cm), where most were also considered to be 'live'. Below this depth, fewer species were present and a larger proportion was considered to be dead.

Our results from the IOM contract area are broadly consistent with those of Goineau and Gooday (2017, 2019) from the UK-1 and OMS contract areas. These were based on a similar methodological approach, namely wet-sorting of multicorer ('megacorer') samples and the inclusion of monothalamids. They confirm that the general characteristics of foraminiferal assemblages are fairly consistent at the shallower eastern end of the CCZ. We limit further comparisons to the Goineau and Gooday (2019) study since this incorporates data from the earlier 2017 paper. The monothalamids predominate in the UK-1/OMS and the IOM samples. Their overall relative abundance is lower in our dataset (62% compared to 80%), although the difference is less when only the 'live' specimens are considered (79% compared to 89%). Among individual groups, *Lagenammina* species and flasks (10%), spheres (16%), and unassigned monothalamids (19%) are all more common in the UK-1/OMS data than in the IOM area (1.5%, 4.3%, 3.4%, respectively). On the other hand, the relative abundance of komokiaceans is considerably higher (32%) than in the UK-1/OMS areas (7%). These differences in the proportions of major groups could reflect the geographical separation between the study areas. However, they are more likely due to the analysis of different size fractions, >150 μm in the UK-1 and OMS areas (upper part of the meiofaunal size range), compared to >250 μm (the macrofaunal size fraction) in the case of the IOM area.

Studies of macrofauna-sized foraminifera from the deep sea are generally fairly rare. In the Pacific, the only ones of which we are aware are those of Bernstein et al. (1978) and Bernstein and Meador (1979), which are based on the >297-μm fraction of box-core sediments from the central North Pacific Climax II site (~28°N, 155°W; 5700–5900 m). As in our study, the foraminifera were almost entirely agglutinated, included large numbers of fragments, as well as species assigned to multichambered genera such as *Hormosina, Reophax, Recurvoides* and *Ammobaculites* and monothalamous genera, notably *Saccammina* and *Thurammina.* In addition to these 'familiar' taxa, the samples yielded large numbers of komokiaceans, although these were not analysed further because of their 'extreme fragility'.

Schröder et al. (1988) presented a taxonomic reassessment of the intact foraminifera in the Bernstein et al. (1978) collection. Despite the greater depth of the Climax II site, some of the species that they illustrate also occur in the IOM samples. These include, among others, *Ammobaculites agglutinans, Cribrostomoides subglobosus, Cystammina galatea, Reticulophragmium trullissatum, 'Reophax'* (= *Hormosinella*) *distans*, *'Reophax'* (= *Hormosinella*) *guttifera,* and the different morphotypes (likely separate species) of *Thurammina papillata.* This is consistent with the wide distribution of many of the common foraminiferal morphospecies across the abyssal Pacific, as discussed further by Gooday et al. (2021).

4.3. Lack of evidence for an experimental impact

A number of *in situ* experiments have been conducted, mainly in the CCZ (OMCO, BIE II, JET, IOM BIE) but also in the SE Pacific (DISCOL study) and the Indian Ocean (INDEX study), to simulate the potential impacts of deep-seabed mining on benthic faunas (summarised by Radziejewska, 2014; Gollner et al., 2017; Jones et al., 2017). A number of factors make these experiments difficult to interpret. Comparisons between them are confounded by differences in methodologies, notably the nature of the impactor. The disturbance itself may not have been uniform, with patches of sediment left undisturbed or only moderately disturbed (Radziejewska, 2014), while samples may sometimes have been taken in the wrong place as a result of imprecise navigation (Jones et al., 2017). The rarity of many species (McClain, 2021; Washburn et al., 2021) can lead to substantial natural small-scale differences in community composition ('patchiness'). The detection of any subtle differences between impacted and control sites persisting after 20 years may therefore require the analysis of unrealistically large numbers of replicate samples (Jumars, 1981). Finally, natural phenomena, such as phytodetritus deposition events, may result in faunal variability over time, further complicating the interpretation of time-series data (Radziejewska, 2002, 2014).

Not surprisingly, given these multiple potential complicating factors, experimental impact studies have yielded somewhat conflicting results (Jones et al., 2017). However, they do generally point to a sharp reduction in faunal densities across many faunal categories, including meiofaunal foraminifera (Kitazato and Okamoto, 1997), in samples taken soon after the experimental disturbance, although post-disturbance density increases were observed in a few groups. Over longer time scales (up to two decades), some groups at some sites exhibited increases in density while others showed no signs of recovery (Jones et al., 2017). Changes in diversity over time were examined in two areas. Macrofaunal polychaete diversity was depressed immediately following the disturbance at the DISCOL site but recovered to some extent over time. Nematode diversity at the species, genus, and family levels was still depressed after 26 years within chain-dredge tracks produced by the OMCO mining consortium in the IFREMER contract area, compared with control samples from areas with and without nodules outside the tracks (Miljutin et al., 2011). However, overall meiofaunal diversity was higher, and evenness lower, compared to background samples (lower right panel in Fig. 5 of Jones et al., 2017).

The present study did not reveal any obvious differences in macrofaunal foraminiferal abundance and assemblage composition at the three IOM BIE sites after 20 years. Species richness and diversity (Fig. 5; Table 8) was consistently higher at the two disturbed sites compared to the control site, although this was not statistically significant. Similar results, albeit over shorter time scales, were reported by Radziejewska (2002, 2014) for metazoan meiofauna from the same sites. Meiofaunal abundances were reduced in samples taken immediately after the July 1995 disturbance. Less than 2 year later (April 1997) they had recovered, but largely because opportunistic nematode and harpacticoid genera had responded to a recent phytodetritus deposition event. In June 2000, densities were similar to those in 1997, although the opportunistic taxa had disappeared. The absence of a clear disturbance impact on foraminifera (after 20 years) and metazoan meiofauna (after 5 years) at the impacted, resedimented and disturbed sites in the IOM BIE area probably reflects some or all of the above-mentioned complicating factors. In addition, although the disturbance created during the IOM BIE by the 'Benthic Disturber' device is designed to mimic seabed mining, including plume generation (Radziejewska, 2014), it was less intense in terms of its impact and spatial scale than the disturbance that will result from commercial operations (Jones et al., 2017).

The practical challenges posed by abyssal macrofaunal foraminifera could also hamper detection of differences between assemblages. In particular, the time-consuming nature of the analyses limits the number of replicates that can realistically be analysed. In the present study, we analysed only three replicates per site, probably far too few to detect all except the most extreme faunal differences between sites (Jumars, 1981). Other problems, notably the tendency of many larger abyssal foraminifera, particularly komokiaceans and tubular monothalamids, to fragment, and the difficulties of distinguishing 'live' from dead specimens, means that specimen counts will be subject to errors that are difficult to assess. A better approach might be to focus on the meiofauna-sized foraminiferal species present in smaller size fractions (>150 μm or >63 μm). These still include many problematic monothalamids (Gooday et al., 2004; Nozawa et al., 2006; Radziejewska et al., 2006; Goineau and Gooday, 2019; Gooday and Goineau, 2019), but they also yield larger proportions of multichambered taxa (globothalamids and tubulothalamids) that are less prone to fragmentation and more amenable to Rose Bengal staining. More time is required to analyse complete replicates for these smaller foraminifera, but this can be alleviated by splitting core samples (Gooday and Goineau, 2019). Analyses

could also be limited to relative species abundances based on picking a standard number of specimens (typically 300), a quick approach often adopted in micropalaeontological research that can greatly increase the number of replicates it is possible to analyse on a realistic time scale (Le et al., 2021). In practice, rapid assessments based on a size- and taxon-related subset of foraminifera, combined with more comprehensive morphological analyses of different size fractions and metabarcoding approaches, may be necessary to detect impacts on the diversity of foraminiferal assemblages and their recovery over time in areas subject to seabed mining impacts.

5. Concluding remarks

Macrofaunal monothalamids are clearly very abundant and diverse in the eastern Clarion-Clipperton Zone, but their role in CCZ ecosystems remains rather obscure (see review of Gooday et al., 2021). A better understanding is emerging of the ecology of one particular group of monothalamids, the xenophyophores, particularly in terms of their growth, provision of habitat structure for other organisms and food uptake (Gooday et al., 2020b; Levin and Rouse, 2020; Tsuchiya and Nomaki, 2021). However, although these giant foraminifera are common across the CCZ, they are not represented in our relatively small samples, which are dominated instead by different kinds of monothalamids, notably delicate komokiaceans (komoki) and tubular macrofauna-sized forms.

The difficulties of distinguishing 'live' from dead specimens, and their tendency to fragment, make evaluating the ecological contribution of these groups particularly problematic. However, it seems likely that groups such as the komoki, many of which have morphologically complex tests, are important in providing small-scale habitat structure for small meiofaunal organisms and eukaryotic microbes. A genetic study by Lecroq et al. (2009) of the komoki genera *Normanina* and *Septuma* offers some evidence for this ecosystem service, which could be provided by dead as well as live specimens. In the latter case, the deployment of pseudopodial nets across and into the surrounding sediments may also have an important influence on other organisms (Bernstein et al., 1978).

In addition to their passive role in providing habitat structure, foraminifera are undoubtedly involved in food webs and carbon cycling on the deep seabed (Gooday et al., 1992, 2021). In general, these protists feed mainly at a low trophic level and are consumed by a variety of specialist and generalist predators. Many abyssal monothalamids accumulate waste pellets composed largely of fine-grained sediment particles, suggesting that they are deposit feeders. They are probably much less active metabolically than their multichambered relatives, particularly the calcareous rotaliids and miliolids, although their abundance suggests a non-trivial contribution to carbon cycling. However, many morphotypes have diffuse cytoplasm making their biomass very low compared to their large body size and also difficult to estimate. Together with growth and respiration rates, biomass is a key metric necessary in order to incorporate monothalamids into abyssal carbon-based food-web models (De Jonge et al., 2020). The fact that these parameters are very poorly constrained severely hampers progress towards understanding the ecological role of monothalamids in the CCZ.

CRediT author statement

Zofia Stachowska-Kamińska Investigation, Data Curation, Writing - Review & Editing. **Andrew J. Gooday** Conceptualization, Methodology, Validation, Data curation, Writing - Original draft preparation, Writing - Reviewing and Editing, Visualization, Supervision. **Teresa Radziejewska** Conceptualization, Formal analysis, Resources, Visualization, Writing - Reviewing and Editing, Project administration. **Pedro Martínez Arbizu** Funding acquisition, Writing - Reviewing and Editing.

Declaration of competing interest

The authors declare the following financial interests/personal relationships which may be considered as potential competing interests: Teresa Radziejewska reports financial support was provided by Polish National Science Centre. Pedro Martinez Arbizu reports financial support was provided by German Ministry of Education and Science (BMBF). T.R. declares that she is an owner of Mar Ecol Consulting, providing consulting services to IOM, a contractor in the CCZ. P.M.A. declares that he is CEO of the company 'INES Integrated Environmental Solutions", providing consultancy services to the German contractor BGR in the CCZ

Data availability

Data will be made available on request.

Acknowledgements

Cruise SO239 was financed by the German Ministry of Education and Science (BMBF) as a contribution to the European project JPI Oceans "Ecological Aspects of Deep-Sea Mining". We acknowledge financial support from the Polish National Science Centre grant No. 2014/13/B/ST10/02996. PMA acknowledges funding from BMBF under contract 03F0707E and 03F0812E. We thank Dr. Brygida Wawrzyniak-Wydrowska for supervising the on-board core processing and the photographs reproduced in Fig. 4A and B, and Ms Aleksandra Kaniak for preparing the map. We are grateful to two anonymous reviewers who provided valuable comments that helped to improve the manuscript considerably.

Appendix A. Supplementary data

Supplementary data to this article can be found online at https://doi.org/10.1016/j.dsr.2022.103848.

References

Bernstein, B.B., Meador, J., 1979. Temporal persistence of biological patch structure in an abyssal benthic community. Mar. Biol. 51, 179–183.
Bernstein, B.B., Hessler, R.R., Smith, R., Jumars, P.A., 1978. Spatial dispersion of benthic Foraminifera in the abyssal central North Pacific. Limnol. Oceanogr. 23, 401–416.
Brockett, T., Richards, C.Z., 1994. Deepsea mining simulator for environmental impact studies. Sea Technol. 35 (8), 77–82.
Chao, A., Chiu, C.H., 2016. Species Richness: Estimation and Comparison. Wiley StatsRef: Statistics Reference Online, pp. 1–26.
Clarke, K.R., Gorley, R.N., 2015. PRIMER v.7. User Manual/Tutorial. PRIMER-E, Plymouth.
Clarke, K.R., Gorley, R.N., Somerfield, P.J., Warwick, R.M., 2014. Change in Marine Communities: an Approach to Statistical Analysis and Interpretation, 3nd edition. PRIMER-E, Plymouth.
De Jonge, D.S.W., Stratmann, T., Lins, L., Vanreusel, A., Purser, A., Marcon, Y., Rodrigues, C.F., Ravara, A., Esquete, P., Cunha, M.R., Simon-Lledó, E., van Breugel, P., Sweetman, A., Soetaert, K., van Oevelen, D., 2020. Abyssal food-web model indicates faunal carbon flow recovery and impaired microbial loop 26 years after a sediment disturbance experiment. Prog. Oceanogr. 189 (102446) https://doi.org/10.1016/j.pocean.2020.102446.
Enge, A.J., Kucera, M., Heinz, P., 2012. Diversity and microhabitats of living benthic foraminifera in the abyssal Northeast Pacific. Mar. Micropal. 96–97, 84–104.
Goineau, A., Gooday, A.J., 2015. Radiolarian tests as microhabitats for novel benthic foraminifera: observations from the abyssal eastern equatorial Pacific (Clarion-Clipperton Fracture Zone). Deep-Sea Res. I 103, 73–85. https://doi.org/10.1016/j.dsr.2015.04.011.
Goineau, A., Gooday, A.J., 2017. Novel benthic foraminifera are abundant and diverse in an area of the abyssal equatorial Pacific licensed for polymetallic nodule exploration. Sci. Rep. 7, 45288 https://doi.org/10.1038/srep.45288.
Goineau, A., Gooday, A.J., 2019. Diversity and spatial patterns of foraminiferal assemblages in the eastern Clarion-Clipperton zone (abyssal eastern equatorial Pacific). Deep-Sea Res. I 149 (103036). https://doi.org/10.1016/j.dsr.2019.04.014.
Gollner, S., Kaiser, S., Menzel, L., Jones, D.O.B., Brown, A., Mestre, N.C., van Oevelen, D., Menot, L., Colaco, A., Canals, M., Cuvelier, D., Durden, J.M., Gebruk, A., Egho, G.A., Haeckel, M., Marcon, Y., Mevenkamp, L., Morato, T., Pham, C.K., Purser, A., Sanchez-Vidal, A., Vanreusel, A., Vink, A., Martínez Arbizu, P.M., 2017. Resilience of benthic deep-sea fauna to mining activities. Mar. Environ. Res. 129, 76–101.

Gooday, A.J., Goineau, A., 2019. The contribution of fine sieve fractions (63-150 μm) to foraminiferal abundance and diversity in an area of the eastern Pacific Ocean licensed for polymetallic nodule exploration. Front. Mar. Sci. 6 (114) https://doi.org/10.3389/fmars.2019.00114.

Gooday, A.J., Levin, L.A., Linke, P., Heeger, T., 1992. The role of benthic Foraminifera in deep-sea food webs and carbon cycling. Pp. 63–91. In: Rowe, G.T., Pariente, V. (Eds.), Deep-Sea Food Chains and the Global Carbon Cycle. [Proceedings of NATO Advanced Research Workshop. College Station, Texas]. Kluwer Academic Publishers, Dordrecht.

Gooday, A.J., Hori, S., Todo, Y., Ohkamoto, T., Kitazato, H., Sabbatini, A., 2004. Soft-walled, monothalamous benthic foraminiferans in the Pacific, Indian and Atlantic Oceans: aspects pf biodiversity and biogeography. Deep-Sea Res I. 51, 33–53.

Gooday, A.J., Goineau, A., Voltski, I., 2015. Abyssal foraminifera attached to polymetallic nodules from the eastern Clarion-Clipperton Fracture Zone: a preliminary description and comparison with North Atlantic dropstone assemblages. Mar. Biodivers. 45, 391–412. https://doi:10.1007/s12526-014-0301-9.

Gooday, A.J., Holzmann, M., Caulle, C., Goineau, A., Kamenskaya, O.E., Weber, A.A.T., Pawlowski, J., 2017. Giant foraminifera (xenophyophores) are exceptionally diverse in parts of the abyssal eastern Pacific where seabed mining is likely to occur. Biol. Conserv. 207, 106–116.

Gooday, A.J., Durden, J.M., Smith, C.R., 2020a. Giant, highly diverse protists in the abyssal Pacific: vulnerability to impacts from seabed mining and potential for recovery. Commun. Integr. Biol. 13, 189–197. https://doi.org/10.1080/19420889.2020.1843818.

Gooday, A.J., Schoenle, A., Dolan, J.R., Arndt, H., 2020b. Protist diversity and function in the dark ocean – challenging the paradigms of deep-sea ecology with special emphasis on foraminiferans and naked protists. Eur. J. Protistol. 75, 125721 https://doi.org/10.1016/j.ejop.2020.125721.

Gooday, A.J., Lejzerowicz, F.J., Goineau, A., Holzmann, M., Kamenskaya, O., Kitazato, H., Lim, S.-C., Pawlowski, J., Radziejewska, T., Stachowska, Z., Wawrzyniak-Wydrowska, B., 2021. The biodiversity and distribution of abyssal benthic foraminifera and their possible ecological roles: a synthesis across the Clarion-Clipperton Zone. Front. Mar. Sci. 8, 634726 https://doi.org/10.3389/fmars.2021.634726.

Gotelli, N.J., Colwell, R.K., 2011. Estimating species richness. In: Magurran, A.E., McGill, B.J. (Eds.), Biological Diversity: Frontiers in Measurement and Assessment. Oxford University Press, pp. 39–54.

Hammer, Ø., Harper, D.A.T., Ryan, P.D., 2001. Past: paleontological statistics software package for education and data analysis. Palaeontologia electronica 4. http://palaeo-electronica.org/2001_1/past/issue1_01.htm.

Jones, D.O.B., Kaiser, S., Sweetman, A.K., Smith, C.R., Menot, L., Vink, A., Trueblood, D., Gremer, J., Billett, D.M.S., Martinez Arbizu, P., Radziejewska, T., Singh, R., Ingole, B., Stratmann, T., Simon-Lledó, E., Durden, J.M., Clark, M.R., 2017. Biological responses to disturbance from simulated polymetallic nodule mining. PLoS ONE 12, e017150. https://doi:10.1371/journal.pone.01717750.

Jumars, P.A., 1981. Limits in detecting and predicting benthic community responses to manganese nodule mining. Mar. Min. 3, 213–229.

Kamenskaya, O.E., Gooday, A.J., Radziejewska, T., Wawrzyniak-Wydrowska, B., 2012. Large, enigmatic foraminiferan-like protists in the eastern part of the Clarion-Clipperton Fracture Zone (abyssal eastern equatorial Pacific): biodiversity and vertical distribution in the sediment. Mar. Biodivers. 42, 311–327. https://doi.org/10.1007/s12526-012-0114-7.

Kaminski, M., 2014. The year 2010 classification of the agglutinated foraminifera. Micropaleontol. 60, 89–108.

Kitazato, H., Okamoto, T., 1997. Responses of foraminiferal distribution in JET – preiminary results. In: Proceedings of International Conference on Environmental Studies for Deep-Sea Mining. Japan November, Tokyo, pp. 20–21, 1997.

Le, J., Levin, L.A., Lejzerowicz, F., Cordier, T., Gooday, A.J., Pawlowski, J., 2021. Scientific and budgetary tradeoffs between morphological and molecular methods for deep-sea biodiversity assessment. Integrated Environ. Assess. Manag. https://doi:10.1002/ieam.4466.

Lecroq, B., Gooday, A.J., Cedhagen, T., Sabbatini, A., Pawlowski, J., 2009. Molecular analyses reveal high levels of eukaryotic richness associated with enigmatic deep-sea protists (Komokiacea). Mar. Biodivers. 39, 45–55.

Levin, L.A., Rouse, G.W., 2020. Giant protists (xenophyophores) function as fish nurseries. Ecology 101, e02933. https://doi.org/10.1002/ecy.2933.

Martínez Arbizu, P., Haeckel, M., 2015. RV SONNE SO239 cruise report/fahrbericht. Berichte GEOMAR Helmholtz-Zentrum Ozeanforschung Kiel. N.Ser., 25. https://doi.org/10.3289/GEOMAR_REP_NS_25_2015.

McClain, C.R., 2021. The commonness of rarity in a deep-sea taxon. Oikos 130, 863–878. http://doi:10.1111/oik.07602.

Miljutin, D.M., Miljutina, M.A., Martínez Arbizu, P.M., Galeron, J., 2011. Deep-sea nematode assemblage has not recovered 26 years after experimental mining of polymetallic nodules (Clarion-Clipperton Fracture Zone, Tropical Eastern Pacific). Deep-Sea Res. I 58, 885–897.

Murray, J.W., 2006. Ecology and Applications of Benthic Foraminifera. Cambridge University Press, Cambridge, New York, Melbourne, Madrid, Cape Town, Singapore, São Paulo.

Nozawa, F., Kitazato, H., Tsuchiya, M., Gooday, A.J., 2006. 'Live' benthic foraminifera at an abyssal site in the equatorial Pacific nodule province: abundance, diversity and taxonomic composition. Deep-Sea Res. I 51, 1406–1422.

Radziejewska, T., 2002. Responses by meiobenthic communities to sediment disturbance simulating the effects of polymetallic nodule mining. Int. Rev. Hydrobiol. 87, 459–479.

Radziejewska, T., 2014. Meiobenthos in the Sub-equatorial Pacific Abyss. A Proxy in Anthropogenic Impact Evaluation. Springer. Heidelberg.

Radziejewska, T., Gooday, A.J., Koltan, M., Szyrwiel, E., 2006. Deep-sea non-calcareous foraminifera: some examples from the Pacific abyssal nodule field. Meiofauna Marina 15, 3–10.

Schröder, C.J., 1986. Deep-wter arenaceous foraminifera of the Northwest Atlantic ocean. Can. Tech. Rep. Hydrogr. Ocean Sci. 71, 1–191 pls 1¬26.

Schröder, C.J., Scott, D.B., Medioli, F.S., Bernstein, B.B., Hessler, R.R., 1988. Larger agglutinated foraminifera: comparison of assemblages from central Pacific and western North Atlantic (Nares abyssal plain). J. Foraminifer. Res. 18, 25–41.

Tendal, O.S., Hessler, R.R., 1977. An introduction to the biology and systematics of Komokiacea. Galathea Rep. 14, 165–194 pls 9–26.

Tsuchiya, M., Nomaki, H., 2021. Rapid response of the giant protist xenophyophores (Foraminifera, Rhizaria) to organic matter supply at abyssal depths revealed by an in situ dual stable isotope labelling experiment. Deep-Sea Res. I 176 (103608). https://doi.org/10.1016/j.dsr.2021.103608.

Voltski, I., Pawlowski, J., 2015. *Flexammina islandica* gen. nov. sp. nov. and some new phylotypes of monothalamous foraminifera from the coast of Iceland. Zootaxa 3964 (2), 245–259.

Washburn, T.W., Menot, L., Bonifácio, P., Pape, E., Błażewicz, M., Bribiesca-Contreras, G., Dahlgren, T.G., Fukushima, T., Glover, A.G., Ju, S.-J., Kaiser, S., Yu, O. H., Smith, C.R., 2021. Patterns of macrofaunal biodiversity across the Clarion-Clipperton Zone: an area targeted for seabed mining. Front. Mar. Sci. 8 (626571) https://doi.org/10.3389/fmars.2021.626571.